NANOSYSTEMS: PHYSICS, CHEMISTRY, MATHEMATICS, 2017, 8 (6), P. 787–792

Synthetic pathway of a Cu_2ZnSnS_4 powder using low temperature annealing of nanostructured binary sulfides

N. S. Kozhevnikova[1], A. S. Vorokh[1], O. I. Gyrdasova[1], I. V. Baklanova[1], A. N. Titov[2,3], M. V. Kuznetsov[1]

[1]Institute of Solid State Chemistry of Ural Branch of Russian Academy of Sciences, 620990, Pervomayskaya str. 91, Ekaterinburg, Russian Federation

[2]Ural Federal University, 620002, Mira str. 19, Ekaterinburg, Russian Federation

[3]Mikheev Institute of Metal Physics of Ural Branch of Russian Academy of Sciences, 620108, S. Kovalevskaya str.18, Ekaterinburg, Russian Federation

kozhevnikova@ihim.uran.ru, vorokh@ihim.uran.ru, gyrdasova@ihim.uran.ru, baklanova@ihim.uran.ru, anti-tov@mail.ru, kuznetsov@ihim.uran.ru

PACS 81.05.Hd, 81.07.Bc, 81.16.Be, 81.10.Jt **DOI 10.17586/2220-8054-2017-8-6-787-792**

Cost-effective route to quaternary Cu_2ZnSnS_4 nanostructured powder fabrication was developed by utilizing a two-step approach. In the first stage, nanostructured binary sulfides Cu_2S, ZnS, and SnS were synthesized by chemical bath deposition. In the second stage, ternary sulfide Cu_2ZnSnS_4 was obtained by low-temperature annealing of binary sulfides' mixtures at 70 and 300 °C. The compounds obtained on both stages were investigated by X-ray diffraction, scanning electron microscopy, optical absorbance and Raman spectroscopy. On the basis of our findings, we established that Cu_2ZnSnS_4 phase has already formed at 300 °C. The synthetic pathway revealed in this work allows reducing the temperature of Cu_2ZnSnS_4 synthesis and as a result, offers the possibility of reducing the manufacturing costs. This work was supported by the Russian Foundation for Basic Research (grant No. 16-03-00566), UrB RAS (grant No.15-20-3-11).

Keywords: nanopowder, CZTS, metal sulfides, low temperature annealing.

Received: 23 November 2017

Revised: 27 November 2017

1. Introduction

Earth abundant kesterite copper-zinc-tin-sulfide Cu_2ZnSnS_4 (CZTS) is considered as cost-effective material for next generation solar cells. CZTS, a quaternary chalcogenide p-type semiconductor, is actively studied as a photovoltaic material due to its high absorption coefficient ($\sim 10^4$ cm^{-1}), optimal direct band energy of ∼1.0–1.5 eV, as well as being composed of naturally abundant and nontoxic elements [1] In other words, CZTS contains non-toxic and cheap Zn and Sn, the production volume of which exceeds 20,000 and 500 times the volume of In production [2]. The similarity of the CZTS crystal structure and physical properties with $CuIn_xGa_{(1-x)}Se_2$ (CIGS) allows production of solar cells by simply replacing the CIGS layer with a CZTS layer without developing a new technology [3–5]. The efficiency increase of solar cells prototypes based on CZTS was increased from 6.7 % [6] in 2009 to 10.1 % in 2011 [4].

The CZTS structure is described both stannite and kesterite [7]. Solid solution range of CZTS is significantly narrower than for CIGS [8]. One-phase powder can be synthesized from a precursor mixture with the elemental ratio: Cu/(Zn+Sn) = 0.92–0.95 and Zn/Sn = 1.0–1.03 [8]. However, in [9] it was assumed that the CZTS solid solution range with the kesterite structure is wider: Cu/(Zn+Sn) = 0.97, and Zn/Sn = 1.42. Higher energy conversion efficiency is demonstrated by CZTS powders, which are "enriched" in zinc and "depleted" in copper [10].

All methods of synthesizing CZTS, as well as CIGS, are traditionally divided into vacuum and non-vacuum procedures. Vacuum methods are based on the deposition of pure elements of atoms, comprising CZTS on a substrate by sputtering [11] or evaporation [12, 13] at certain pressures These methods require complex equipment and high power consumption, which leads to higher costs for the synthesized compounds. In order to reduce a production technology cost, non-vacuum deposition methods such as spraying with pyrolysis, electrochemical deposition, chemical bath deposition, are used. These techniques have been developed in the production of semiconductor CIGS and CdTe thin films [14] and now can be used for the synthesis of CZTS [15–18]. Chemical bath deposition method allows easy regulation of the reagent concentrations and the deposition time.

CZTS structure can be obtained by annealing at 55 °C [19]. According to this, the main limitation of chemical bath deposition method is that the temperature of the bath water cannot exceed 90–95 °C. In this study we propose decreasing the synthetic temperature by a two-step approach. In the first stage, nanostructured binary sulfides Cu_2S, ZnS, and SnS are synthesized by chemical bath deposition. In the second stage, ternary sulfide Cu_2ZnSnS_4

was obtained by low-temperature annealing of binary sulfides' mixtures at different temperatures. The compounds obtained at both stages were investigated by X-ray diffraction, scanning electron microscopy, optical absorbance and Raman spectroscopy.

2. Methods

Synthesis of the initial copper sulfide Cu_xS was carried out by the interaction of a soluble $CuSO_4$ salt using thiourea N_2H_4CS as the sulfur source. The initial concentration of $CuSO_4$ and N_2H_4CS were 0.01 and 0.03 M, respectively. Based on the concept of reversibility of the N_2H_4CS hydrolytic decomposition in aqueous alkaline solutions, the reaction was carried out at pH = 11.35 and temperature 70 °C for 2.5 hours. The pH was adjusted by adding aq. NH_4OH to the initial solution of $CuSO_4$. After synthesis, the Cu_xS powder was filtered, washed with 0.1 M aq. NH_4OH and distilled water, and air-dried at room temperature.

The initial zinc sulfide powder ZnS was obtained by reaction of 0.02 M aq. $ZnSO_4$ with 0.1 M aq. sodium thiosulfate $Na_2S_2O_3$. The reaction was carried out at pH = 6 and temperature 90 °C for 27 hours. The prolonged reaction time was due to the kinetic factor of decomposition of the sulfur source, $Na_2S_2O_3$. The obtained ZnS powder was also filtered, washed by distilled water and air-dried at room temperature.

To synthesize the initial SnS_x tin sulfide, 0.01 M aq. $SnCl_2$ and 0.05 M aq. sodium sulfide Na_2S were used. In aqueous solutions Sn^{2+} ions usually undergo hydrolysis; to suppress this process, the synthesis of SnS_x was carried out at pH 0.46 in a solution of ethylenediaminetetraacetic acid (EDTA, 0.01 M). The reaction mixture temperature in the SnS_x synthesis was 70 °C, the deposition time was 3 hours. After synthesis, the resulting SnS_x powder was filtered and air-dried at room temperature.

Besides, the used pH values allowed obtaining not only the basic phases of the sulfides, but also a phase containing crystalline elemental sulfur.

The second stage is synthesis of the ternary sulfide Cu_2ZnSnS_4 by annealing the corresponding amounts of individual sulfides obtained at the first stage. Based on the X-ray phase analysis data, weights of 2 moles of CuS, 1 mole of ZnS and 1 mole of SnS_x were calculated. The sulfides CuS, ZnS and SnS_x were mixed, ground and pressed into tablets. The obtained tablets were annealed *in vacuo* at 70 °C for two weeks and 300 °C for two days. Elemental sulfur S_8 in the initial powders allowed us to conduct annealing experiments without the need for adding extra crystalline sulfur to the initial mixture.

X-ray diffraction (XRD) patterns of all composites were obtained using a Stadi automatic diffractometer with CuK_α ($\lambda = 1.5406$ Å) with 2θ angle step 0.03 ° and exposure time of 40 sec. Scanning electron microscopy (SEM) was carried out in order to analyze the microstructure and morphology of all synthesized samples using JEOL-JSM LA 6390. To confirm the change in bandgap, the UVVis spectra in the wavelength range of 300–700 nm ($BaSO_4$ was used as the standard) of composites were recorded using Shimadzu UV-2401 PC spectrophotometer. The chemical composition of the samples was determined by two methods: (*i*) by the energy-dispersive X-ray analysis (EDX) using a JEOL-JSM LA 6390 electron microscope with a JED 2300 analyzer; (*ii*) by X-ray photoelectron spectrometry (XPS) using ESCALAB MKII electron spectrometer with MgK_α (E = 1253.6 eV) irradiation beam The Raman spectra of the samples were obtained at room temperature on a RENISHAW-1000 spectrometer ($\lambda = 532$ nm, $P = 25$ mW).

3. Results and discussion

The phase composition, crystal structure and particle size (coherent scattering regions) of the individual sulfides synthesized at the first stage were studied by X-ray diffraction analysis. According to the diffraction data, Cu_xS powder contains 81 % CuS, 3 % Cu_2S, 16 % $CuSO_4$(wt %). The content of initial salt $CuSO_4$ in the Cu_xS powder is explained by insufficient washing of the obtained Cu_xS after the reaction. The particle size of CuS was 10.6 nm. Zinc sulfide powder consists of the main ZnS phase 78 % and 22 % sulfur S_8. The ZnS particle size was 4.6 nm. The synthesized powder SnS_x was a mixture of phases: 10 % SnS, 23 % SnS_2, 14 % SnO, 53 % S_8. The presence of tin oxide SnO was due to the impossibility to suppress the Sn^{2+} ions hydrolysis process.

The powder annealed at 70 °C differs from initial mixture by presence of $Cu_5Sn_2S_7$ phase (Fig. 1). This indicates that formation of CZTS began from the intercalation of tin into the Cu_xS matrix.

Currently, different methods are required to characterize the crystal structure and compositional purity of CZTS nanoparticles obtained by the annealing at 300 °C. Fig. 2 demonstrates the SEM images and XRD pattern. The EDX measurements revealed the compositional non-stoichiometry within the quaternary sulfide nanopowder. Therefore, CZTS particles have different structures. The XRD pattern (Fig. 2b) proved two binary sulfides CuS and SnS_2 to present in the CZTS powder as impurities. The CZTS phase cannot be identified by X-ray diffraction unambiguously, because three main peaks of ZnS and CTS coincide with three peaks of CZTS phase. Presence

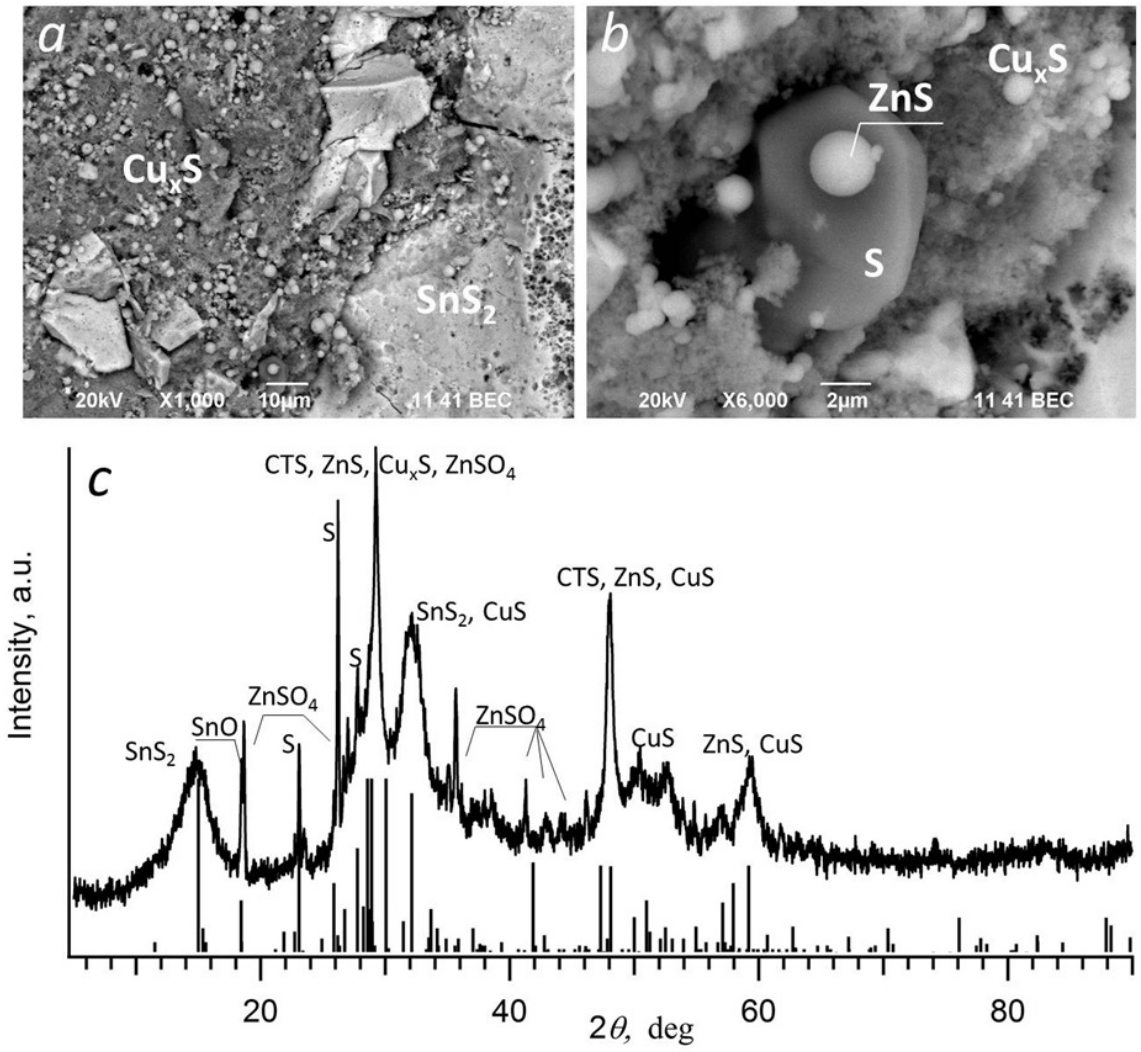

FIG. 1. a, b – SEM images of CZTS sample annealed at 70 °C. The composition of marked regions was determined by EDX analysis; c – XRD pattern of CZTS sample annealed at 70 °C. The main peaks are marked as belonging to phases CuS, CuS_2, ZnS, $ZnSO_4$, SnS_2, SnO, $Cu_5Sn_2S_7$ (CTS)

of CZTS phase was determined by Raman shift spectroscopy (Fig. 3a). The most intense peak at 329 cm^{-1} corresponds to kesterite structure [20, 21]. The small peaks at 248, 289 and 370 cm^{-1} could be referred to as 'shoulders' of the main peak. It is important that the ZnS and CTS phases were not present in the Raman spectrum. This fact allowed the interpretation that the most intensive XRD peaks belong to the CZTS phase. According to X-ray diffraction analysis, the resulting powder was a mixture of Cu_2ZnSnS_4:SnS_2:CuS phases, predominantly CZTS in a ratio of 96:2:2. The particle size of Cu_2ZnSnS_4 was ∼100 nm.

The optical measurements are consistent with the XRD analysis and Raman spectroscopy data. Three inflections are visible in the optical absorption curve (Fig. 3). This indicates that the powder consists of three phases. In order to determine the effective band gap E_g of each phase, the experimental absorption spectra were reduced to the form $(\alpha h\nu)^2 = f(h\nu)$. Bandgap of 1.7 eV could be attributed to either Cu_2ZnSnS_4 or SnS_2 [22], 1.3 eV – to CuS, and 1.2 eV – to SnS. Increasing of the band gap to 1.7 eV in comparison to $E_g \approx 1.5$ eV for bulk Cu_2ZnSnS_4 [23] may be due to either small particle size (100 nm), or to the ratio of [Sn]/[Cu] in CZTS. According to experimental data [24], an increase in the fraction of [Sn] can lead to an increase in E_g for Cu_2ZnSnS_4 films up to 1.63 eV, but the mechanism of this phenomenon has not been studied yet.

Analysis of the stoichiometric ratios for the elements was carried out using XPS spectrometry. The XPS spectrum from the surface of the powder annealed at 300 °C is shown in Fig. 4. Apart from, the XPS measurements

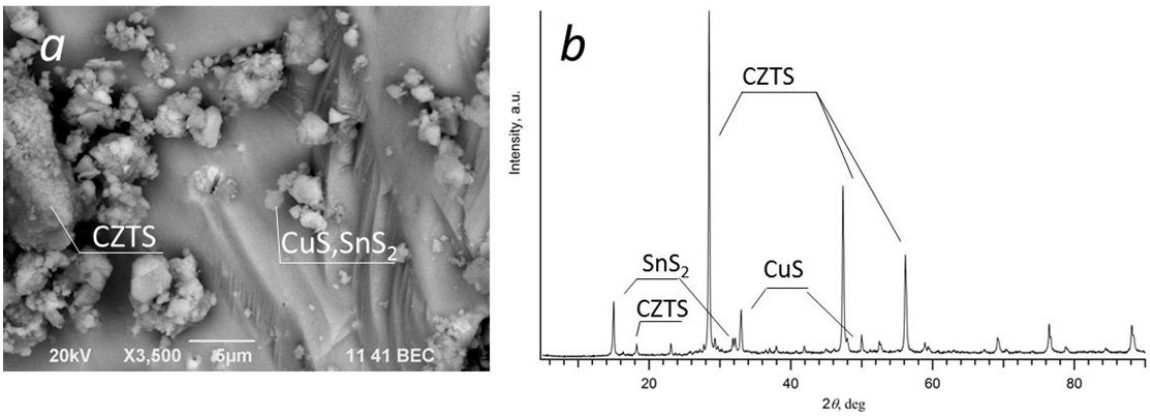

FIG. 2. a – SEM images of CZTS sample annealed at 300 °C. The composition of marked regions was determined by EDX analysis; b – XRD pattern of CZTS sample annealed at 300 °C

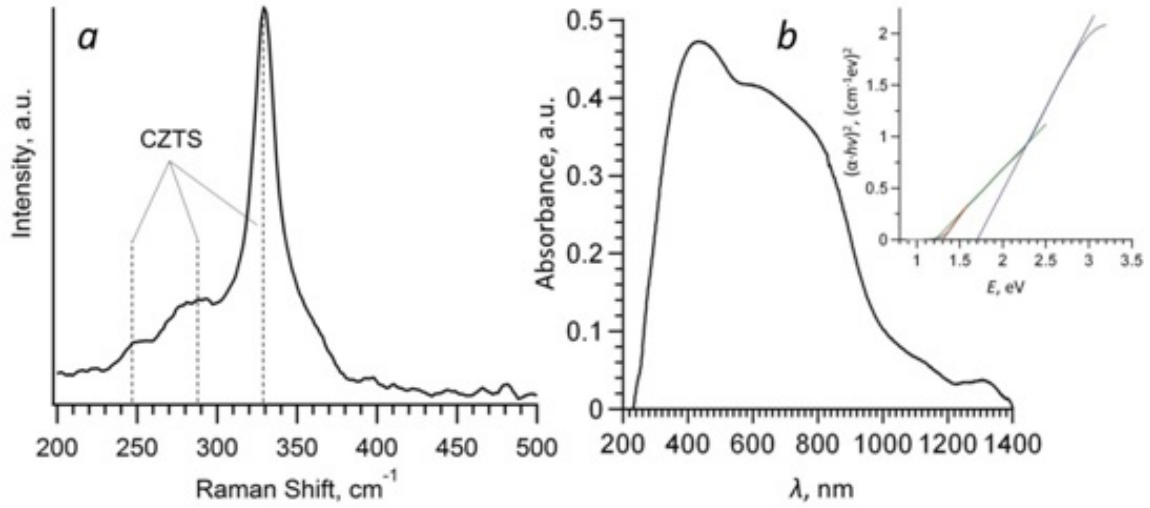

FIG. 3. Raman spectra (a) and optical absorbance (b) of CZTS sample annealed at 300 °C. In the inset: the Tauc plot was used for Eg determination. Eg (Cu_2ZnSnS_4) = 1.7 eV, Eg (CuS) = 1.3 eV, Eg(SnS) = 1.2 eV

were made after etching the sample by an argon beam. The etching led to removal of surface impurities. The elemental composition was quantified by measuring the partial area under the peaks: (i) in the case of metals (Cu, Zn, Sn) - according to the detailed XPS spectrum (right-hand insert in Fig. 4); (ii) in the case of sulfur according to the review spectrum. The results are shown by histogram (left-hand insert in Fig. 4).

The penetration sample depth of the XPS analysis is several nanometers. In contrast, the EDX chemical analysis allows a depth of about one micron within a local area. In order to compare these methods, elemental composition of the CZTS particle, shown in Fig. 2a, was investigated by using both XPS and EDX analyses. In its turn, the XRD data refer to the entire volume of the sample. Thus, the elemental composition analysis fulfilled by using all methods mentioned above made it possible to determine the distribution of metals and sulfur within synthesized nanopowder of quaternary sulfide.

The chemical composition data obtained by different methods are given in the Table 1. It can be seen from the Table that the Cu content on the surface is smaller than in the bulk. On the other hand, the Sn content is larger on the surface than in the bulk. This experimental fact could be explained by the suggestion that the tin-containing impurity phases are located mainly on the surface of the sample.

Obviously, the stoichiometry of the sample changes strongly both while moving from the surface into the bulk, and from the local area to the entire volume of the sample. According to EDX, there is a lack of tin and sulfur in a separate CZTS particle. The XRD data reveals that the powder composition has an exact stoichiometric ratio

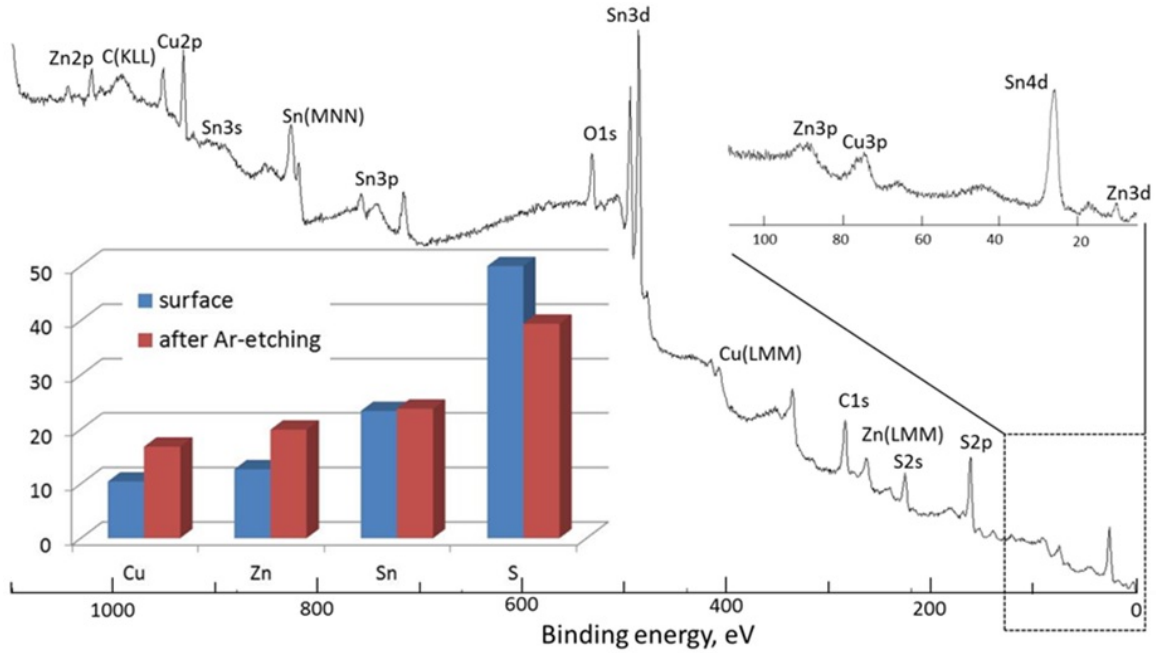

FIG. 4. Survey XPS spectrum for CZTS powder annealed at 300 °C. In the right-hand inset: detailed XPS spectrum of 0–110 eV range. In the left-hand inset bar chart of element content calculated from XPS data

TABLE 1. Chemical composition within nanopowder of quaternary sulfide CZTS synthesized at 300 °C obtained by XPS, EDX and XRD methods

Content	XPS-surface	XPS-Ar_20min etching	EDX, CZTS particle	XRD
Cu, at%	10.4	16.8	31.6	22.2
Zn, at%	12.7	19.9	15.5	15.8
Sn, at%	23.4	23.8	12.7	11.7
S, at%	53.5	39.4	40.2	50.3
Stoichiometry				
Cu/(Sn+Zn)	0.29	0.38	1.12	0.81
Zn/Sn	0.54	0.84	1.22	1.35
S/(Cu+Zn+Sn)	1.15	0.65	0.67	1.01

between metals and sulfur, but an excess of Zn is observed among metals. In its turn, the Raman spectroscopy data proved the absence separate Zn-containing phase, so Zn may be assumed to enter the CZTS lattice. In this case, the stoichiometric composition of the powder can be written approximately as follows: $Cu_{2-x}Zn_{1+x}SnS_4$, $x \approx 0.3$.

4. Conclusion

Thus, the use of nanocrystalline sulfides CuS, ZnS and SnS_x as intermediate compounds may lead to a decrease in the solid-phase synthesis temperature from the traditional 550 °C to 300 °C and the formation of Cu_2ZnSnS_4 in the nanocrystalline state. On the basis of our findings, we established that Cu_2ZnSnS_4 phase had already formed at 300 °C. The synthetic pathway revealed in this work allows reduction of the temperature at which Cu_2ZnSnS_4 synthesis occurs, and as a result, offers the possibility of reducing the manufacturing costs. Finally, it is apparent that the creation of compositionally uniform and stoichiometric multinary CZTS semiconductor nanoparticles requires further study.

Acknowledgments

This work was supported by the Russian Foundation for Basic Research (grant No. 16-03-00566), Ural Branch of Russian Academy of Sciences (grant No. 15-20-3-11), and was carried out in accordance with the scientific and research plans and state assignment of the ISSC UrB RAS (AAAA-A16-116122810214-9, AAAA-A16-116122810209-5).

References

[1] Tan J.M.R., Lee Y.H., Pedireddy S., Baikie T., Ling X.Y., Wong L.H. Understanding the Synthetic Pathway of a Single-Phase Quarternary Semiconductor Using Surface-Enhanced Raman Scattering: A Case of Wurtzite Cu_2ZnSnS_4 Nanoparticles. *J. Am. Chem. Soc.*, 2014, **136**(18), P. 6684–6692.

[2] USGS, Commodity Statistics and Information, USGS Minerals Information, 2010. URL: http://minerals.usgs.gov/minerals/pubs/commodity/.

[3] Choubrac L., Lafond A., Guillot-Deudon C., Moëlo Y., Jobic S. Structure flexibility of the Cu_2ZnSnS_4 absorber in low-cost photovoltaic cells: from the stoichiometric to the copper-poor compounds. *Inorg. Chem.*, 2012, **51**(6), P. 3346–3348.

[4] Barkhouse D.A.R., Gunawan O., Gokmen T., Todorov T.K., Mitzi D.B. Device characteristics of a 10.1% hydrazine-processed $Cu_2ZnSn(Se,S)_4$ solar cell. *Prog. Photovolt: Res. Appl.*, 2012, **20**, P. 6–11.

[5] Bag S., Gunawan O., Gokmen T., Zhu Y., Todorov T.K., Mitzi D.B. Low band gap liquid-processed CZTSe solar cell with 10.1% efficiency. *Energy Environ. Sci.*, 2012, **5**, P. 7060–7065.

[6] Katagiri H., Jimbo K., Maw W.S., Oishi K., Yamazaki M., Araki H., Takeuchi A. Development of CZTS-based thin film solar cells. *Thin Solid Films*, 2009, **517**(7), P. 2455–2460.

[7] Hall S.R., Szymanski J.T., Stewart J.M. Kesterite $Cu_2(Zn\ Fe)SnS_4$ and stannite $Cu_2(FeZn)SnS_4$ structurally similar but distinct minerals. *Can. Mineral.*, 1978, **16**, P. 131–137.

[8] Muska K., Kauk M., Altosaar M., Pilvet M., Grossberg M., Volobujeva O. Synthesis of Cu_2ZnSnS_4 monograin powders with different compositions. *Energy Procedia*, 2011, **10**, P. 203–207.

[9] Nozaki H., Fukano T., Ohta S., Seno Y., Katagiri H., Jimbo K. Crystal structure determination of solar cell materials: Cu_2ZnSnS_4 thin films using X-ray anomalous dispersion. *J. Alloys Comp.*, 2012, **524**, P. 22–25.

[10] Katagiri H., Jimbo K., Tahara M., Araki H., Oishi K. The influence of the composition ratio on CZTS-based thin film solar cells. *MRS Proceedings*, 2009, P. 1165.

[11] Ito K., Nakazawa T. Electrical and optical properties of stannite-type quaternary semiconductor thin films. *Japan. J. Appl. Phys.*, 1988, **27**(11R), P. 2094.

[12] Katagiri H., Ishigaki N., Ishida T., Saito K. Characterization of Cu_2ZnSnS_4 thin films prepared by vapor phase sulfurization. *Japan. J. Appl. Phys.*, 2001, **40**(2R), P. 500.

[13] Tanaka T., Kawasaki D., Nishio M., Guo Q., Ogawa H. Fabrication of Cu_2ZnSnS_4 thin films by co-evaporation. *Phys. Stat. Sol. C*, 2006, **3**(8), P. 2844–2847.

[14] Hibberd C.J., Chassaing E., Liu W., Mitzi D.B., Lincot D., Tiwari A.N., Hibberd C.J., Chassaing E., Liu W., Mitzi D.B., Lincot D., Tiwari A.N. Non-vacuum methods for formation of $Cu(In,Ga)(Se,S)_2$ thin film photovoltaic absorbers. *Prog. Photovolt.: Res. Appl.*, 2010, **18**, P. 434–452.

[15] Nakayama N., Ito K. Sprayed films of stannite Cu_2ZnSnS_4. *Appl. Surf. Sci.*, 1996, **92**, P. 171–175.

[16] Kamoun N., Bouzouita H., Rezig B. Fabrication and characterization of Cu_2ZnSnS_4 thin films deposited by spray pyrolysis technique. *Thin Solid Films*, 2007, **515**(15), P. 5949–5952.

[17] Kumar Y.B.K., Babu G.S., Bhaskar P.U., Raja V.S. Preparation and characterization of spray-deposited Cu_2ZnSnS_4 thin films. *Sol. Energy Mater. Solar Cells*, 2009, **93**(8), P. 1230–1237.

[18] Kumar Y.B.K., Babu G.S., Bhaskar P.U., Raja V.S. Effect of starting-solution pH on the growth of Cu_2ZnSnS_4 thin films deposited by spray pyrolysis. *Phys. Stat. Sol. A*, 2009, **206**(7), P. 1525–1530.

[19] Scragg J.J., Dale P.J., Peter L.M. Towards sustainable materials for solar energy conversion: preparation and photoelectrochemical characterization of Cu_2ZnSnS_4. *Electrochem. Comm.*, 2008, **10**(4), P. 639–642.

[20] Sun L., He J., Kong H., Yue F., Yang P., Chu J. Structure, composition and optical properties of Cu_2ZnSnS_4 thin films deposited by Pulsed Laser Deposition method. *Solar Energy Materials & Solar Cells*, 2011, **95**, P. 2907–2913.

[21] Guc M., Levcenko S., Bodnar I.V., Izquierdo-Roca V., Fontane X., Volkova L.V., Arushanov E. Pérez-Rodríguez A. Polarized Raman scattering study of kesterite type Cu_2ZnSnS_4 single crystals. *Sci Rep.*, 2016, **6**, P. 19414.

[22] Cifuentes C., Botero M., Romero E., Calderón C., Gordillo G. Optical and structural studies on SnS films grown by co-evaporation. *Braz. J. Phys.*, 2006, **36**(3b), P. 1046–1049.

[23] Sarswat P.K., Free M.L. A study of energy band gap versus temperature for Cu_2ZnSnS_4 thin films. *Physica B: Cond. Mat.*, 2012, **407**(1), P. 108–111.

[24] Malerba C., Biccari F., Ricardo C.L.A.,Valentini M., Chierchia R., Müller M., Santoni A., Esposito E., Mangiapane P., Scardi P., Mittiga A. CZTS stoichiometry effects on the band gap energy. *J. Alloys and Compounds*, 2014, **582**, P. 528–534.